

A Hybrid Enhanced Independent Component Analysis Approach for Segmentation of Brain Magnetic Resonance Image

Shaik Basheera^{#,*}, and M. Satya Sai Ram[@]

[#]*Acharya Nagarjuna College of Engineering and Technology, Acharya Nagarjuna University, Guntur-522 510. Andhra Pradesh, India*

[@]*Chalapathi Institute of Engineering and Technology, Guntur-522 019, Andhra Pradesh, India*

^{*}*E-mail: basheer_405@rediffmail.com*

ABSTRACT

Medical imaging and analysis plays a crucial role in diagnosis and treatment planning. The anatomical complexity of human brain makes the process of imaging and analyzing very difficult. In spite of huge advancements in medical imaging procedures, accurate segmentation and classification of brain abnormalities remains a challenging and daunting task. This challenge is more visible in the case of brain tumors because of different possible shapes of tumors, locations and image intensities of different types of tumors. In this paper we have presented a method for automated segmentation of brain tumors from magnetic resonance images. An enhanced and modified Gaussian mixture mode model and the independent component analysis segmentation approach has been employed for segmenting brain tumors in magnetic resonance images. The results of segmentation are validated with the help of segmentation evaluation parameters.

Keywords: Gaussian mixture mode; Segmentation

1. INTRODUCTION

Brain tumors remain one of the most common brain diseases that has affected and devastated many lives. According to data available with International Agency for Research on Cancer (IARC), India ranks second for occurrence and mortality of brain cancers as of the year 2012. Medical image segmentation being a complex and challenging task needs precise methods for identifying and segmenting different regions of interest. Especially in case of brain which has a specifically complex structure, its precise segmentation of structures is of most importance. Magnetic resonance imaging (MRI) is an important diagnostic imaging technique for the early detection of abnormal changes in tissues and organs. It possesses good contrast resolution for different tissues and has advantages over computerised tomography (CT) for brain studies due to its superior contrast properties⁵. Therefore, the majority of research in medical image segmentation of Brain concerns MR images. Also MRI are examined by radiologists based on visual interpretation of the films to identify the presence of tumor and other abnormal tissue. The shortage of radiologists and the large volume of MRI to be analysed make such readings labor intensive, cost expensive and often inaccurate. The sensitivity of the human eye in interpreting large numbers of images decreases with increasing number of cases, particularly when only a small number of slices are affected. Hence there is a need for automated systems for analysis of such medical images.

The literature presents a gamut of MRI segmentation approaches, most of the approaches fall under thresholding, region growing, clustering and hybrid approaches^{1,2}. Image segmentation based on thresholding is one of the oldest and powerful technique, since the threshold value divides the pixels in such a way that pixels having intensity value less than threshold belongs to one class while pixels whose intensity value is greater than threshold belongs to another class³. Segmentation based on edge detection attempts to resolve image by detecting the edges between different regions that have sudden change in intensity value are extracted and linked to form closed region boundaries. Region based methods⁴, divides an image into different regions that are similar according to a set of some predefined conditions. The neural network based image segmentation techniques reported in the literature⁵ can mainly be classified into two categories: supervised and unsupervised methods. Clustering is an unsupervised learning technique, where one needs to know the number of clusters in advance to classify pixels⁶. A similarity condition is defined between pixels, and then similar pixels are grouped together to form clusters. The hybrid approaches⁷ employ any two of the above methods and are characterised by the application for which they are adopted. These hybrid methods utilise advantages of those two methods and avoid inherent limitations. Some of the recent works reported in the literature are presented as follows Chaudhari⁸, *et al.* presented pixel classification based brain magnetic resonance Images segmentation. The authors performed automatic segmentation of brain into four classes namely background, cerebrospinal fluid, grey and white matter.

Roy and Maji⁹, proposed an unsupervised and knowledge based skull stripping algorithm for brain magnetic resonance imaging termed as S3, which is based on brain anatomy and image intensity characteristics. The authors used adaptive intensity thresholding followed by morphological operations for increased robustness. Moeskops¹⁰, *et al.* described a method for automatic segmentation of magnetic resonance brain images into a number of tissue classes using a convolution neural networks. Pereira¹¹, *et al.* described an automatic segmentation method based on Convolution Neural Networks (CNN), exploring small 3×3 kernels. The authors used intensity normalisation as a preprocessing step, which proved together with data augmentation to be very effective for brain tumor segmentation in magnetic resonance images. Nandi¹² presented the detection of human brain tumor using magnetic resonance image segmentation and morphological operators. Then morphological operators along with basic image processing techniques were used for separating tumor cells from normal cells. Chandra and Balasingham¹³ presented the detection of brain tumor and localisation of a deep brain RF source using microwave imaging. They author used Levenberg-Marquadt iterative scheme as microwave imaging technique to solve the inverse scattering problem for the head of the phantom in 403.5 MHz medical radio band. The simulation results showed that at least 45dB SNR was required for small tumor detection. The authors presented a localisation method based on microwave imaging for deep brain RF source. Abhay¹⁴, *et al.* proposed a semi-supervised clustering technique that used the concepts of multi objective optimisation for segmentation of magnetic resonance brain image in intensity space. The intensity values of brain pixels were utilised as the features. A modern multi objective optimisation technique based on the concept of simulated annealing was used to optimise the three cluster validity indices. The performance of the approach was compared with other techniques like FCM, Expectation maximisation, fuzzy-VGAPS clustering techniques. Jambholkar¹⁵, *et al.* proposed an Empirical wavelet transform (EWT) method for feature extraction of brain SPECT image and also assisted in brain tumor detection. EWT decomposed the image into a number of sub-band images and fuzzy c-mean (FCM) clustering algorithm was used for segmentation to achieve higher accuracy. Support vector machine was used as a classifier. Adhikari¹⁶, *et al.* presented a spatial fuzzy C-means (SPFCM) algorithm for segmentation of magnetic resonance images. They employed spatial information from the neighborhood of each pixel and realised by defining a probability function. The resulted SPFCM algorithm solved the problem of sensitivity to noise and intensity inhomogeneity in magnetic resonance imaging data and improved the segmentation results. The authors showed that SPFCM was superior in performance when compared to some FCM based algorithms. Gonal and Kohir¹⁷, proposed a classification method that classifies brain magnetic resonance images as normal or abnormal by using wavelets texture features and k-means classifier. The Euclidean distances measured between feature vectors of test magnetic resonance image and reference magnetic resonance image were fed to k-means classifier for classification. Praveen and Agrawal¹⁸ presented a four phase

hybrid approach for brain tumor detection and classification in magnetic resonance images. The image pre-processing includes noise filtering and skull detection as the first phase. Feature extraction using gray level co-occurrence matrix was the second phase. The third phase dealt with normal or abnormal classification of inputs by using least square support vector machine classifier with multilayer perception kernel. The authors used fast bounding box for segmentation of tumor. The classification accuracy was found to be 96.63 per cent. Handore and Kokare¹⁹ described the performance analysis of various methods of tumor detection. The authors described comparative study of various methods for tumor detection. The authors showed that image segmentation plays an important role in medical imaging. They also described that segmentation can work efficiently in detecting and extracting the tumor from magnetic resonance Image.

In the proposed approach an improved K -means algorithm and EM algorithm are combined to formulate a hybrid strategy for better clustering. The proposed approach aims to exploit the capability of providing well distributed cluster of K-means and the compactness of clusters provided by EM. The initial clusters are provided by the improved K-means algorithm. This initial clustering operation results in centers which are widely spread in the given data. These centers form the initial variable for EM, which subsequently uses these variables and iterates to find the local maxima. This is subsequently used for enhancing and modifying Gaussian Mixture Mode Model and the ICA segmentation approach that follows it. The performance of the segmentation approaches is evaluated using different performance measures they are Probabilistic Rand Index (PRI)²⁰, Variation of Information (VOI)²¹, Global Consistency Error (GCE)²⁰, Peak Signal to Noise Ratio (PSNR)²², and Jaccard Distance (JD)²².

2. MATERIAL AND METHOD

Blind source separation by independent component analysis has shown significant applications in the domain of signal processing, medical signal processing and medical image processing. Over the years, many types of computer systems assisted methods have been developed and implemented for analysing magnetic resonance images. The methods include Eigen image analysis, principal component analysis (PCA) and Fuzzy C Means (FCM) method. Eigen image analysis are found to be more effective in segmentation and feature extraction while the performance of neural network appears to be satisfactory in segmenting brain tissues. These methods provide better performance when compared to the classical maximum likelihood methods. With the advent of multi spectral images different segmentation and analysis procedures based on orthogonal subspace projection, kalman filter etc., have evolved over a period of time. But the typical issue with these procedures is the requirement of prior knowledge. In this context segmentation approach based on independent component analysis (ICA) which is an unsupervised texturing method provides greater advantage in the segmentation of brain tissues.

One typical disadvantage of ICA is its assumption that the sources are independent. In order to relax this assumption, the

concept of mixture models have been introduced. In the case of mixture model, the observed data is characterised into several mutually exclusive classes. To improve the generalisation performance of ICA it is imperative to choose a proper search space.

Given a set $\{x_i, i = 1, 2, \dots, N\}$, where x_i is the gray value of the i^{th} image pixel modeled as i.i.d and N is the total number of the image pixels. GMM assumes a mixture model consisting of c Gaussian density components with the parameters $\theta_k = \{u_k, \Sigma_k\}$ in the k^{th} component. In GMM, the probability density of x_i is formulated by

$$p(x_i|\pi, \theta) = \sum_{k=1}^c \pi_k p(x_i | \theta_k) \tag{1}$$

where $\theta = \{\theta_1, \theta_2, \dots, \theta_c\}$ is the parameters of all the components and π_k is the mixing weight of the k^{th} component, satisfying $\pi_k \geq 0$ and $\sum_{k=1}^c \pi_k = 1$. The k^{th} Gaussian is denoted by

$$p(x_i|\theta_k) = \frac{1}{\sqrt{(2\pi)^d |\Sigma_k|}} \exp\left(-\frac{(x_i - u_k)^T \Sigma_k^{-1} (x_i - u_k)}{2}\right)$$

where u_k and Σ_k are the mean and the covariance matrix, respectively. The parameters $\{\theta, \pi\}$ can iteratively be estimated by maximising the likelihood function using the proposed hybrid Expectation-Maximisation.

In the proposed improvement, a computationally less complex approach is suggested to identify better initial clusters thereby enhancing the efficiency and performance of the clustering operation. The steps involved in the implementation of the improved K-means clustering are mentioned as follows.

- Step 1: Considering middle point in each data set as the initial centroids
- Step 2: Computing the Euclidean distance for each data point from the origin
- Step 3: Sorting the obtained data point using the distance computed
- Step 4: Portioning the sorted data points in to K equal sets
- Step 5: Considering the middle point in each set as the initial centroid
- Step 6: Computing the distance between each data point to the all the initial centroids
- Step 7: Finding the closest centroid c_j and assign d_j to cluster j for each data point d_i
- Step 8: Setting the Cluster $Id[i] = j // j : d_i$ of the closest cluster
- Step 9: Setting the nearest $Dist[i] = d(di, c_j)$
- Step 10: Recalculate the centroids for each cluster $j(1 \leq j \leq k)$
- Step 11: For each data point d_i , its distance from the centroid of the present nearest cluster is calculated. If this distance is less than or equal to the present nearest distance, the data point stays in the same cluster. The operation moves to step for every centroid $c_j(1 \leq j \leq k)$ the distance $d(di, c_j)$ is computed.
- Step 12: If convergence criteria are met then giving the clusters or going back to Step 2.

In EM, alternating steps of expectation (E) and maximisation (M) are performed iteratively till the results converge. The E step computes an expectation of the likelihood by including the latent variables as if they were observed, and maximisation (M) step, which computes the maximum likelihood estimates of the parameters by maximising the expected likelihood found on the last E step. The parameters found on the M step are then used to begin another E step, and the process is repeated until convergence.

Mathematically for a given training dataset $\{x(1), x(2), \dots, x(m)\}$ and model $p(x, z)$

where z is the latent variable, we have:

$$l(\theta) = \sum_1^m \log p(x; \theta) \tag{3}$$

$$= \sum_1^m \log \sum_z p(x; z; \theta) \tag{4}$$

As can be seen from the above equation, the log likelihood is described in terms of x, z and θ . But since z , the latent variable is not known, we use approximations in its place. These approximations take the form of E & M steps mentioned above and formulated mathematically as follows.

E Step, for each i :

$$Q_{(i)}(Z^{(i)}) := P(z^{(i)} | x^{(i)}; \theta) \tag{5}$$

M Step, for all z :

$$\theta := \arg \max_{\theta} \sum_i \sum_{z^{(i)}} Q_{(i)}(z^{(i)}) \log \frac{p(x^{(i)}, z^{(i)}; \theta)}{Q_{(i)}(z^{(i)})} \tag{6}$$

where $Q_{(i)}$ the posterior distribution of $z^{(i)}$ given the $(x^{(i)})$'s conceptually.

To incorporate the spatial information into GMM, as a typical variation of GMM is proposed by using the MRF model as a prior. Different from GMM, each pixel i in modified GMM is characterised by its probability vector $\pi_i = (\pi_i^1, \pi_i^2, \dots, \pi_i^c)^T$ where π_i^k denotes the probability of the i^{th} pixel belonging to the k^{th} cluster. In modified GMM, the corresponding mixture model of x_i is assumed as

$$p(x_i|\pi, \theta) = \sum_{k=1}^c \pi_i^k p(x_i | \theta_k) \tag{7}$$

where $p(x_i|\theta_k)$ is a Gaussian distribution with parameters $\theta_k = \{u_k, \Sigma_k\}$, to take the spatial dependence into account, the prior distribution of π is given by the MRF model through a Gibbs density function

$$p(\pi) = \exp \frac{-\beta \sum_{i=1}^N V_{N_i}(\pi)}{Z} \tag{8}$$

where Z is a normalising constant and β is regularisation parameter. $V_{N_i}(\pi)$ is the clique potential function of the pixel label vectors π_m within the neighborhood N_i of the i^{th} pixel

$$V_{N_i}(\pi) = \sum_{m \in N_i} |\pi_i - \pi_m|^2 \tag{9}$$

Notice that the $\pi = \{\pi_1, \pi_2, \dots, \pi_k\}$ in GMM is shared by all

pixels, whereas in modified GMM π_i is different for each pixel i and depends on its neighboring pixels. In modified GMM, the modified EM algorithm is utilised to obtain the maximum a posteriori (MAP) estimation of the parameters. The above will be considered as source for the ICA for further implementation of segmentation.

3. EVALUATION OF SEGMENTATION

The performance of the proposed segmentation approach is evaluated using different performance measures they are probabilistic rand index (PRI), variation of information (VOI), global consistency error (GCE), peak signal to noise ratio (PSNR), dice coefficient (DCE) and jaccard distance (JD).

The PRI²⁰ counts the fraction of pairs of pixels whose labeling are consistent between the computed segmentation and the ground truth, averaging across multiple ground truth segmentations to account for scale variation in human perception. Consider a set of manually segmented (ground truth) images $\{S_1, S_2, \dots, S_K\}$ corresponding to an image $X = \{x_1, x_2, \dots, x_i, \dots, x_N\}$, where a subscript indexes one of N pixels. S_{test} is the segmentation of a test image, and then PRI is defined as:

$$PR(S_{test}, \{S_k\}) = \frac{1}{N} \sum_{ij} \left[(I_i^{S_{test}} = I_j^{S_{test}}) p_{ij} + I(I_i^{S_{test}} \neq I_j^{S_{test}})(1 - p_{ij}) \right] \quad (10)$$

$$p_{ij} = \frac{1}{k} \sum_{ij} I(I_i^k = I_j^k) \quad (11)$$

The GCE²⁰ measures the extent to which segmentation can be viewed as a refinement of the other. Segmentations which are related in this manner are considered to be consistent, since they could represent the same natural image segmented at different scales. Let S and S' be two segmented images, for a given point x_i (pixel), considering the classes (segments) that contain x_i in S and S' . These sets are denoted in the form of pixels by $C(S, x_i)$ and $C(S', x_i)$ respectively. The local refinement error (LRE) is then defined at point x_i as:

$$LRE(S, S', x_i) = \frac{|C(S, x_i) \setminus C(S', x_i)|}{|C(S, x_i)|} \quad (12)$$

The GCE forces all local refinements to be in the same direction and is defined as:

$$GCE(S, S') = \frac{1}{N} \min\{LRE(S, S'; x_i), LRE(S', S, x_i)\} \quad (13)$$

The VoI²¹ metric defines the distance between two segmentations as the average conditional entropy of the segmentation given the other, and thus roughly measures the amount of randomness in the segmentation which cannot be explained by the other. A clustering with clusters X_1, X_2, \dots, X_k is represented by a random variable X with $X = \{1 \dots K\}$ such that $p_{i=|X_i|/n}$ and $n = \sum X_i$ the variation of information between two clusters X and Y can be given by

$$V_I(X; Y) = H(X) + H(Y) - 2I(X, Y) \quad (14)$$

where $H(X)$ is entropy of X and $I(X, Y)$ is mutual information

between X and Y . The mutual information of two clustering is the loss of uncertainty of one clustering if the other is given.

The PSNR²² is used to find the deviation of segmented image and from the ground truth image. Equation (6) represents the PSNR. In this equation mean squared error (MSE) for two $M * N$ monochrome images f and z and it is given by Eqn. (16). Max Bits gives the maximum possible pixel value (255) of the image.

$$PSNR = 10X \log_{10} \frac{MaxBits^2}{MSE} \quad (15)$$

$$MSE = \frac{1}{M \times N} \sum_{x=0}^{M-1} \sum_{y=0}^{N-1} ((f(x, y) - z(x, y))^2) \quad (16)$$

The JD²² which measures dissimilarity between sample sets is complementary to the Jaccard coefficient and is obtained by subtracting the Jaccard coefficient from Eqn. (1). The Jaccard index, also known as the Jaccard similarity coefficient is a statistic used for comparing the similarity and diversity of sample sets. The Jaccards Coefficient is given by

$$J = \frac{|A \cap G|}{|A \cup G|} \quad (17)$$

The Jaccards distance is given by

$$JD = 1 - J \quad (18)$$

where A and G are two set of data points

The DCE²³ measures the spatial overlap between two segmentations. Conceptually that DCE is also a special case of the kappa statistic commonly used in reliability analysis. It is commonly used in reporting performance of segmentation.

$$DCE = \frac{2|A \cap G|}{|A| + |G|} \quad (19)$$

where A and G are two set of data points.

4. RESULTS AND DISCUSSION

The following section summarises the results of the proposed segmentation approach. The proposed was coded in Matlab R 2012 an and the validity of the segmentation is demonstrated with the help of evaluation parameters. The ground truth images for validation were obtained through manual segmentation. The following source images listed in Fig. 1 have been considered for testing and validation. To have a true representation the images are of different sizes and intensity values.

The histogram profile of the images serves to give a trend in distribution of intensity values and help in the initial stages of the choosing the threshold. The histogram of the images is illustrated in the Figs. 2 (a)- 2(c).

The histogram profile clearly illustrates that the test image has different intensity profile and variant pixel distribution. This pixel distribution is also influenced the type and the location of the tumor too. Similarly, the size of the tumor also plays a crucial role in defining the intensity profile. The intensity profile of a particular region can also give an inclination towards percentage of scattered elements.

Edge detection refers to the progression of identify and

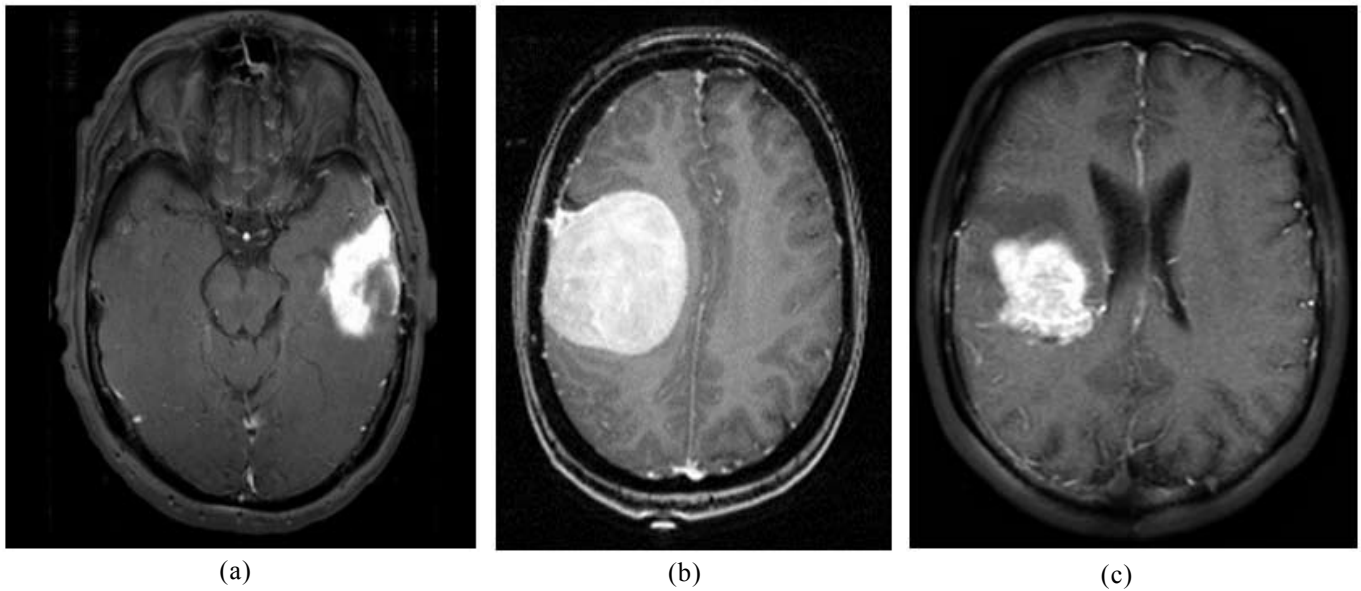
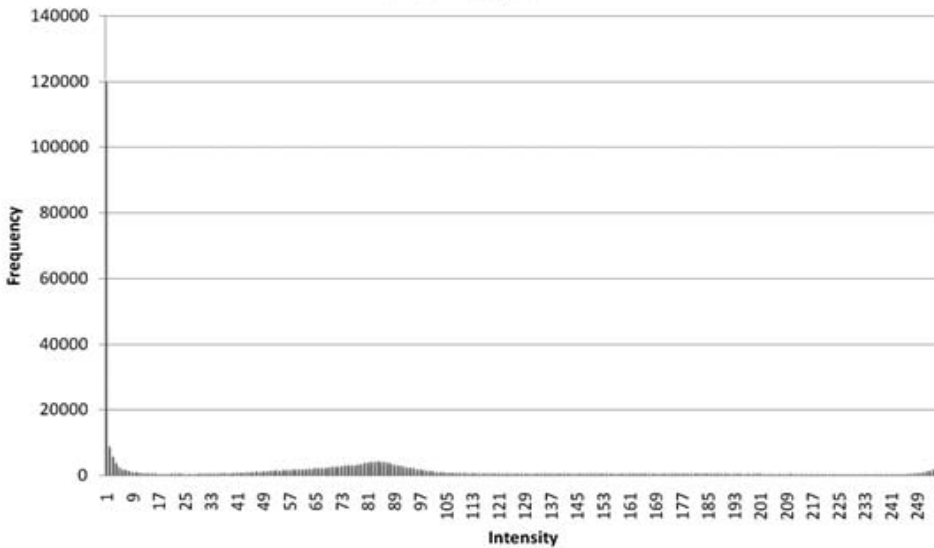
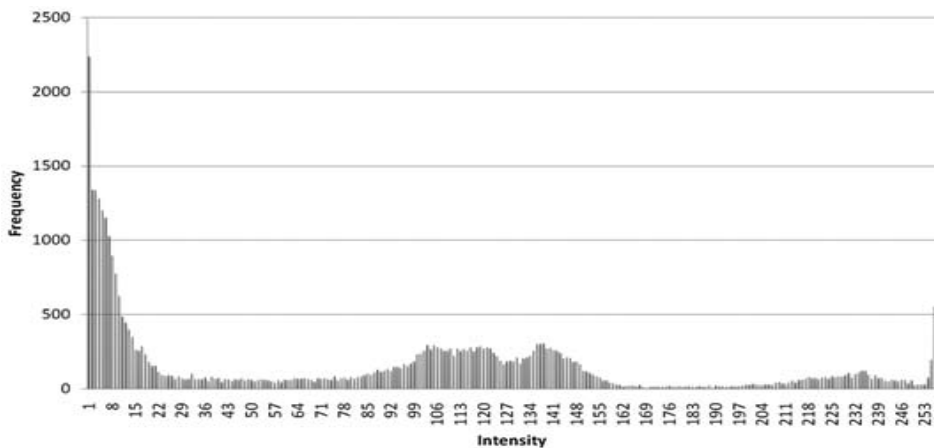


Figure 1. Image (a), (b) and (c) considered for evaluation.



(a)



(b)

locate sharp discontinuities in an image.

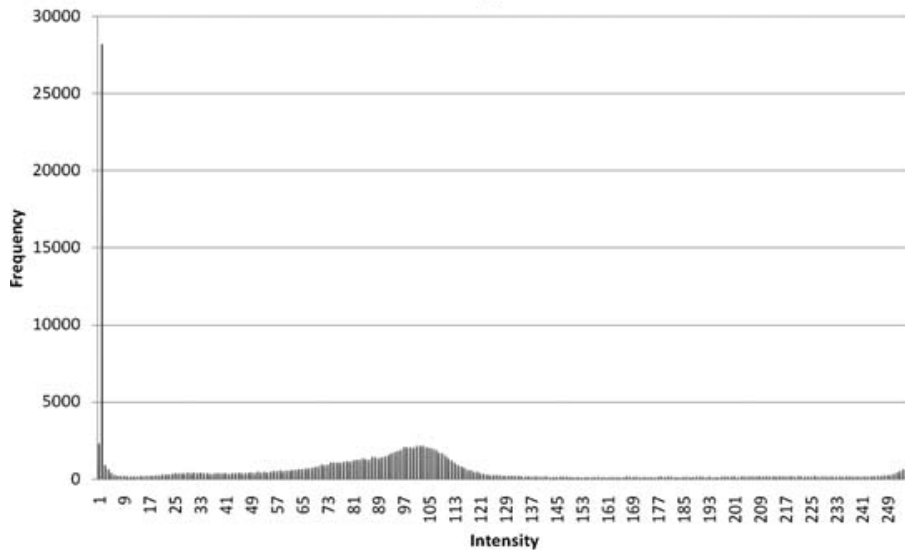
Edge is a basic and important feature of an image. Image is a combination of edges. Detecting edges is one of the mainly significant features in image segmentation. Edge detection is a vital step as it is a process of identifying and locates sharp discontinuities in a representation. The edges of the test images as identified using Prewitt edge detector is illustrated through Fig. 3.

The complexity of medical image segmentation can be clearly understood from the above images. Even though we are using a similar edge detector we can see an appreciable difference in performance between different images. It can be clearly observed that the edges are neatly demarcated in image (b) where as in image (c) the edges appeared to merge and in the case of image (a) it appears to be cluttered and distorted.

It can be observed from the intensity profile and edges that test images present a very complicated task for segmentation. The results of the segmentation of these test images using the proposed approach are depicted using the Figs. 4(a)- 4(c).

Through Figs. 4(a) - 4(c) can be clearly observed through visual inspection that the proposed approach has delivered a neat and clean segmentation. The performance is clearly visible in Fig. 4(a) and Fig. 4(c), while in Fig. 4(b) we can observe that some of the background elements have also been included in the

segmented image.



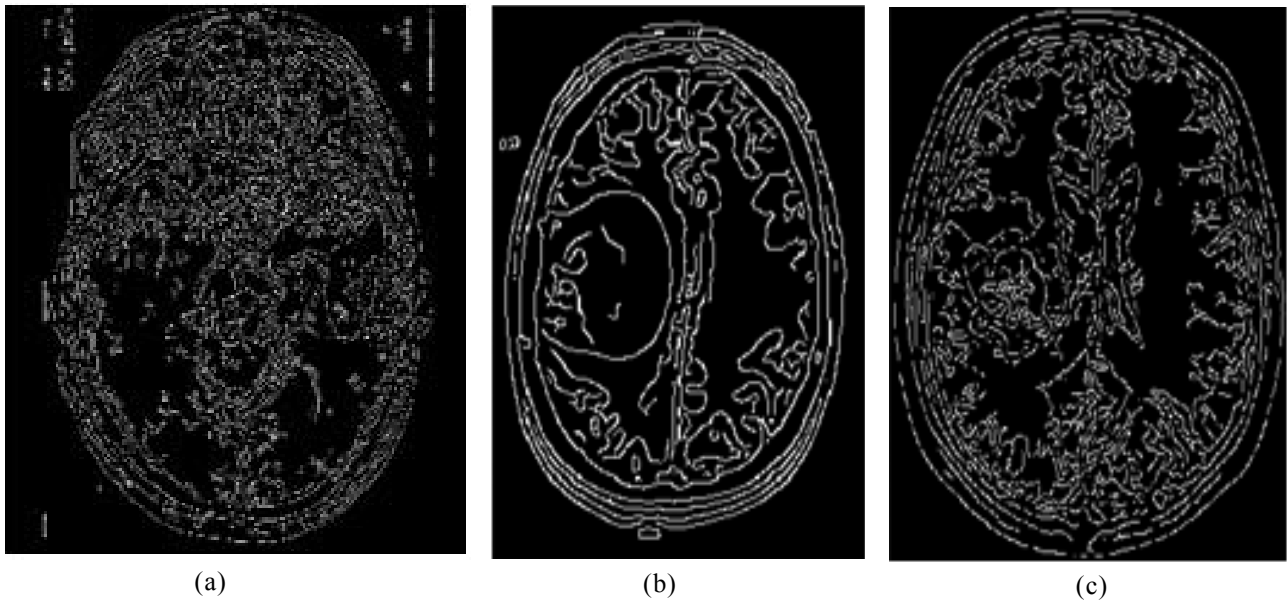
(c)

Figure 2. Histograms of images of figure 1 (a), 1(b), and 1(c).

To illustrate the effectiveness of the segmentation a sample illustration of intensity profiling of the segmented tumor of image 1(b) is given in the Fig. 5. It can be clearly observed from the figure there is a neat distribution of the segmentation indicating clear profiling.

The validity of the segmentation is evaluated through evaluation parameters discussed in section 4, these are computed by comparing the segmented image with the ground truth obtained using manual segmentation. The results of evaluation are listed using the Table 1.

From the Table 1, it can be inferred that the proposed method has delivered in terms of all the evaluation parameters. It is also interesting to observe that the image 1(a) which produced cluttered has in fact been segmented better than the other two images as evident from the evaluation

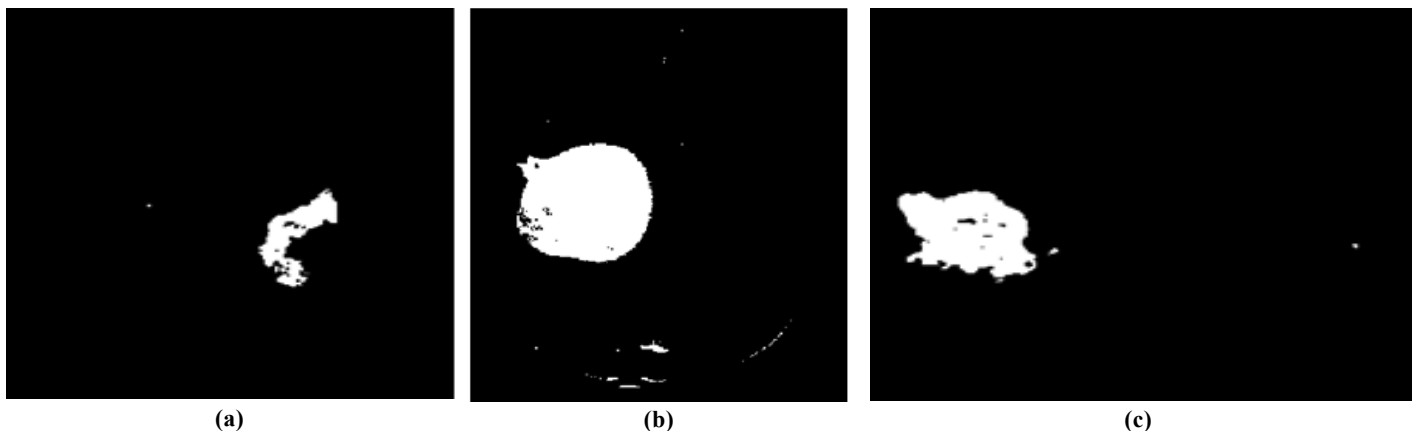


(a)

(b)

(c)

Figure 3. The edges identified for test images using Prewitt operator.



(a)

(b)

(c)

Figure 4. Tumor in image (a), (b), and (c) were segmented using the proposed approach.

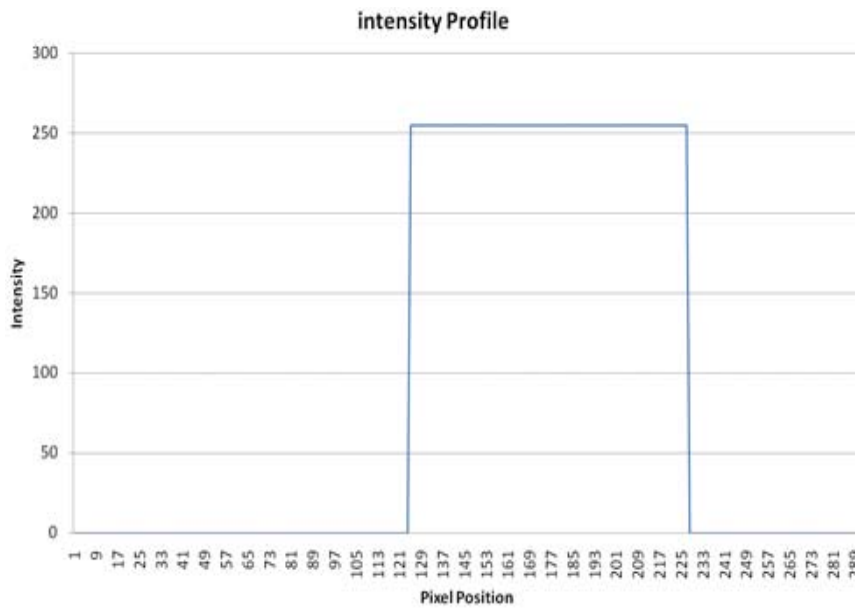


Figure 5. Intensity profile distribution for segmented image of 1(b).

existing Gaussian mixture mode models in the form of a hybrid expected maximum (EM) algorithm which can result in the formation of better initial clusters. Similarly, the incorporation of Markov random field (MRF) will account for variations in spatial information. This enhances the performance of ICA by incorporating the designed Modified Gaussian mixture mode model. The above approach can be used for segmentation and subsequent analysis of different neurological disorders and can be useful in delivering clinically significant results. In order to illustrate the performance of the segmentation approach it has been evaluated using different performance measures like PRI, VOI, GCE, PSNR, DCE, and JD. The performance measures amply illustrate the capability of proposed method in delivering better segmentation.

parameters.

The overlap images of ground truth images and the segmented images illustrated using Fig. 6 also clearly points to near perfect segmentation achieved with the help of the proposed approach.

5. CONCLUSION

It can be safely concluded that the proposed approach provides better segmentation of brain tumors. Some of the important contributions are modifications to

REFERENCES

1. Dass, Rajeshwar; Priyanka & Devi, Swapna. Image segmentation techniques. *Int. J. Electron. Comm. Technol.*, 2012, 3(1), 66-70.
2. Pal, N.R. & Pal, S.K. A review on image segmentation techniques. *Pattern Recognition*, 1993, 26(9), 1277-94. doi: 10.1016/0031-3203(93)90135-J
3. Kang, W.X.; Yang, Q. & Liang, R. The comparative research on image segmentation algorithms. *In IEEE Conference on ETCS*, 2009, 703-707.

Table 1. Evaluated evaluation parameters for the proposed segmentation approach

Image	PRI	VOI	GCE	DCE	JD	JD	PSNR
Image (a)	0.994077	0.0410444	0.00415916	4.11438e-06	0.830311	0.169689	62.1516
Image (b)	0.968306	0.234687	0.0124698	7.54947e-08	0.879389	0.120611	45.5802
Image (c)	0.994581	0.0413095	0.00459764	9.83213e-07	0.91453	0.0854701	60.1518

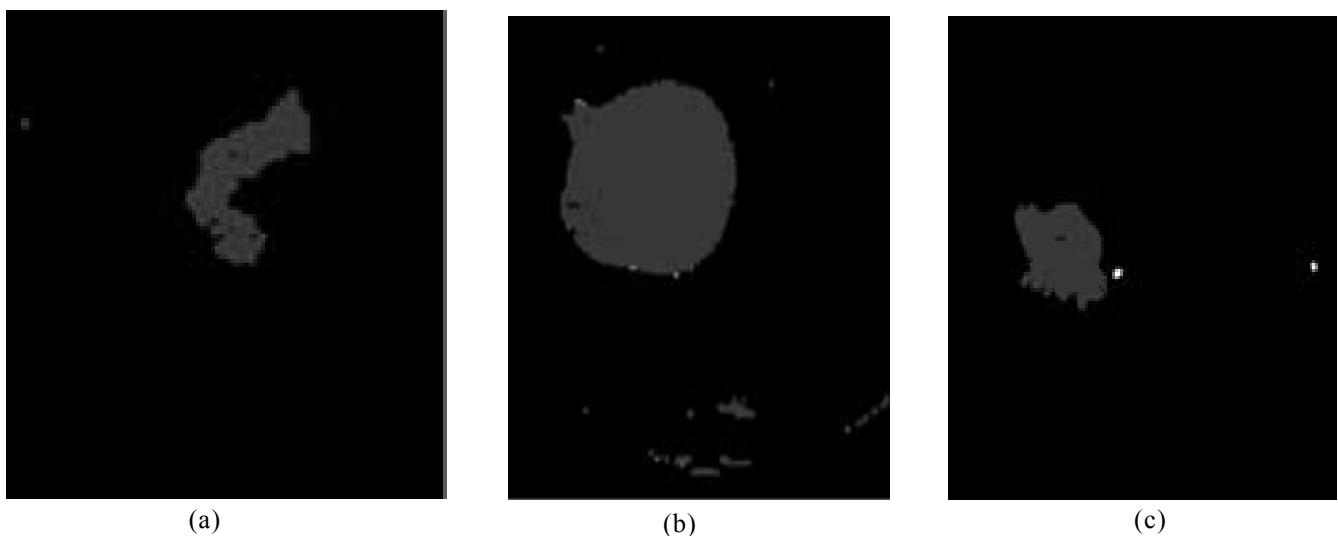


Figure 6. Overlap images of segmented images with ground truth images.

- doi: 10.1109/ETCS.2009.417
4. Kaganami, H.G. & Beij, Z. Region based detection versus edge detection. *IEEE Trans. Intel. Inf. Hiding Mult. Signal Proc.*, 2009, 1217-21.
doi: 10.1109/IIH-MSP.2009.13
 5. Zhu, Changming; Ni, Jun; Li, Yanbo & Gu, Guochang. General tendencies in segmentation of medical ultrasound images. *In International Conference on ICICSE*, 2009, 113-117.
doi: 10.1109/ICICSE.2009.71
 6. Dehariya, V. K.; Shrivastava, S.K. & Jain, R.C. Clustering of image data set using k-means and fuzzy k-means algorithms. *In International Conference on CICN*, 2010, 386- 391.
doi: 10.1109/CICN.2010.80
 7. Ozisik, D. Post-earthquake damage assessment using satellite and aerial video imagery. Dissertation thesis, University of Twente. 2004
 8. Chaudhari, A.; Pawar & Kulkarni, J. Pixel classification based brain MR image segmentation. *In International Conference Industrial instrumentation and control (ICIC)*, Pune, 2015, 462-465.
doi: 10.1109/IIC.2015.7150786
 9. Roy, S. & Maji, P.A. Simple skull stripping algorithm for brain MRI. *In Eighth International Conference on Advances in pattern recognition (ICAPR)*, 2015, 1-6.
doi: 10.1109/ICAPR.2015.7050671.
 10. Pim, Moeskops.; Viergever, Max A.; Mendrik, Adriënne M.; Linda, S. De Vries; Manon, J.; Benders, N.L. & Ivana, Işgum. Automatic segmentation of MR brain images with a convolution neural network. *IEEE Trans. Med. Imag.*, 2016, **35**(2), 1252-1261.
doi: 10.1109/TMI.2016.2548501
 11. Pereira, S.; Pinto, A.; Alves, V. & Silva, C.A. brain tumor segmentation using convolution neural networks in MRI images. *IEEE Trans. Med. Imaging*, 2016, **35**(5), 1240-1251.
doi: 10.1109/TMI.2016.2538465
 12. Nandi, A. Detection of human brain tumor using MRI image segmentation and morphological operators. *In IEEE International Conference on Computer Graphics Vision and Security (CGVIS information)*, Bhubaneswar, 2015, 55-60.
doi: 10.1109/CGVIS.2015.7449892
 13. Chandra, R. & Balasingham, I. Detection of brain tumor and localisation of a deep brain RF source using microwave imaging. *In 9th European Conference on Antennas and Propagation (EuCAP)*, Lisbon, 2015, 1-5.
 14. Abhay, K.; Alok; Sriparna, Saha & Ekbal, Asif. MR brain image segmentation using multi-objective semi-supervised clustering. *In IEEE International Conference Signal Processing Information Communication Energy System (SPICES)*, Kozhikode, 2015, 1-5.
doi: 10.1109/SPICES.2015.7091468
 15. Jambholkar, T; Gurve, D; & Sharma, P.B. Application of empirical wavelet transform (EWT) on images to explore brain tumor. *Signal processing computing and control (ISPCC)*, Wagnaghat, 2015, 200-204.
doi: 10.1109/ISPCC.2015.7375025
 16. Adhikari, S.K.; Sing, J.K.; Basu, D.K. & Nasipuri, M.A. Spatial fuzzy C-means algorithm with application to MRI image segmentation. *In Eighth International Conference on Advances in pattern recognition (ICAPR)*, Kolkata, 2015, 1-6.
doi: 10.1109/ICAPR.2015.7050691.
 17. Gonal, J.S. & Kohir, V.V. Classification of brain MR images using wavelets texture features and k-Means classifier. *In International Conference on Electrical, Electronics, Signals, Communication and Optimisation (EESCO)*, Visakhapatnam, 2015, 1-5.
doi: 10.1109/EESCO.2015.7253749.
 18. Praveen, G.B. & Agrawal, A. Hybrid approach for brain tumor detection and classification in magnetic resonance images. *Communication, control and intelligent systems (CCIS)*, Mathura, 2015, 162-166.
doi: 10.1109/CCIntelS.2015.7437900.
 19. Handore, S. & Kokare, D. Performance analysis of various methods of tumour detection. *In International Conference on Pervasive Computing (ICPC)*. Pune, 2015, 1-4.
 20. Hanbury, A. & Stottinger, J. On segmentation evaluation metrics and region count. *In 19th International Conference on Pattern Recognition*, 2008 Tampa, FL, USA, 2008, 8-11.
doi: 10.1109/ICPR.2008.4761582
 21. Chinnadurai, V.K.; Damayanti, G. & Chandrashekar. Improved level set method for segmentation and grading of brain tumors in dynamic contrast susceptibility and apparent diffusion coefficient magnetic resonance images. *Int. J. Engg. Sc. Technol.*, 2010, **2**(5), 1461-1472.
 22. Padamavati, S.; Subashini, P. & Sumi, A. Empirical evaluation of suitable segmentation algorithm for IR images. *Int. J. Comp. Sc. Issues*, 2010, **7**(4), 22-29.
 23. Francisco, J.; Estrada; Allan, D. & Jepson. Quantitative evaluation of a novel image segmentation algorithm. *In IEEE Computer Society Conference*, 2005, 2, 1132-39.

CONTRIBUTORS

Mr Shaik Basheera, received the B.Tech (Electronics and Communication Engineering) from JNTUH, Hyderabad and M.Tech (Digital Systems and Computer Electronics) from JNTUA, Anapatur, Currently pursuing his PhD from Acharya Nagarjuna University, Guntur. His area of research is Medical image and machine learning.

His contribution is doing experiment, collecting data, performing simulation and writing paper.

Dr M. Satya Sai Ram, received his B.Tech, M.Tech from Acharya Nagarjuna University and PhD from JNTUH Hyderabad. He is currently working as Professor Department of ECE, Chalapathi Institute of Engineering and Technology, LAM, Guntur. He is guiding many research scholars in the area of signal and image processing. He has contributed in collecting data, planning the experiment, preparing paper and editing paper.